Journal of Russian Laser Research, Volume 34, Number 4, July, 2013

DIAGNOSTICS OF A POTASSIUM PLASMA PRODUCED BY VISIBLE AND IR NANOSECOND LASER ABLATION

M. Salik,[1]* M. Hanif,[2] J. Wang,[1] and X. Q. Zhang[1]

[1]*Institute of Optoelectronics*
Beijing Jiaotong University
Beijing 100044, China

[2]*MCS (National University of Sciences & Technology)*
Rawalpindi 46000, Pakistan

*Corresponding author e-mail: 12119009@bjtu.edu.cn

Abstract

We present spectroscopic emission studies of a laser-produced potassium plasma generated by the fundamental mode (1064 nm) and the second harmonic (532 nm) of a *Q*-switched pulsed Nd:YAG laser. The spectra predominantly reveal the spectral lines of neutral potassium. We use experimentally observed line profiles of neutral potassium to determine the excitation temperature using Boltzmann plots, and the Stark-broadened line profiles to determine the electron-number density. We also study variations in the excitation temperature and electron-number density as functions of the laser irradiance.

Keywords: potassium, laser ablation, optical emission spectroscopy, plasma temperature, electron density.

1. Introduction

Laser-induced breakdown spectroscopy (LIBS) is a technique where the output from a pulsed laser is focused onto a certain sample to create an intense plasma. This sensitive technique is based on optical detection of certain atomic and molecular species by monitoring their emission signals from the laser-induced plasma. It provides a useful method to determine the chemical composition of a wide range of materials including metals, liquids, aerosols, plastics, minerals, biological tissues, etc. [1–4]. It is a simple analytical technique as compared to many other types of elemental analysis because of its straightforward experimental setup. In this technique, one requires a pulsed laser for generating a microplasma on the target surface, and elemental analysis is accomplished by studying the emission of the plasma plume. The laser-induced-plasma characteristics depend upon several parameters, which include the features of the target, properties of the ambient medium, laser wavelength and pulse duration, etc. First direct spectral analysis made by LIBS can be attributed to Runge et al. [5]; however, this technique is increasingly used as an analytical method in research [6, 7].

Potassium is an important and unique element due to its chemical properties. It has been extensively studied using the LIBS technique. Measures et al. [8] have studied the electron density and temperature elevation of a potassium-seeded plasma by laser resonance pumping. Thomas et al. [9] studied the film

Manuscript submitted by the authors in English on March 11, 2013.

coating that inhibits the spin relaxation of polarized potassium atoms. Konjevic et al. [10] have measured the experimental Stark width and shift for spectral lines of neutral and ionized atoms. Yilmaz et al. [11] studied the pulsed laser deposition of stoichiometric potassium tantalite niobate films from segmented evaporation targets. Resonantly enhanced frequency doubling of an 820 nm GaAlAs diode laser in a potassium lithium niobate crystal was reported by Reid et al. [12]. Davis et al. [13] studied the excess noise acquired by a laser beam propagating through an atomic potassium vapor. Zahn et al. [14] studied a mesopause temperature profiling by a potassium lidar. Nystrom et al. [15] reported the microstructure of epitaxial potassium niobate thin films prepared by metal organic chemical vapor deposition. Monitoring of urea and potassium by reverse iontophoresis in vitro was studied by Wascotte et al. [16].

In this work, we extend the studies of the laser-produced potassium plasma using the fundamental (1064 nm) and second (532 nm) harmonics of a Nd:YAG laser. We determine the excitation temperature and electron-number density at different positions along the propagation direction and at different laser irradiances. The aim of the present work is to exploit the LIBS technique to inspect the plasma generated on the surface of commercially available potassium using the fundamental mode and the second harmonics of a nanosecond Nd:YAG laser. Extracted information on the number density and plasma temperature is useful for deposition of potassium thin films using the pulsed laser deposition technique discussed in [11, 13, 15].

2. Experimental Details

2.1. The Sample

In our experiment, the sample under study is potassium (K) containing mass percentage of 59.19. A small amount of the sample was used to prepare a pellet of 15 mm diameter and 3 mm thickness with the help of a hydraulic press machine using a load of 10 t for a time duration of 5 min. The SEM photograph of the potassium is shown in Fig. 1 a, and the quantitative analysis of the sample conducted by JSM-6490A analytical scanning electron microscope (SEM) is shown in Fig. 1 b.

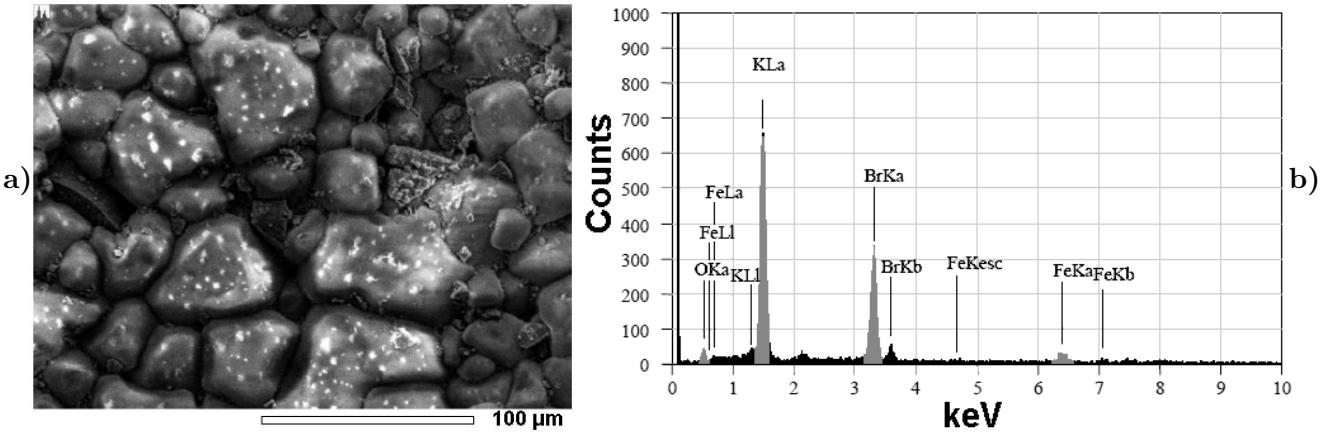

Fig. 1. SEM photograph of a potassium sample showing its morphology (a) and the SEM signals of the potassium sample (b).

2.2. Experimental Setup

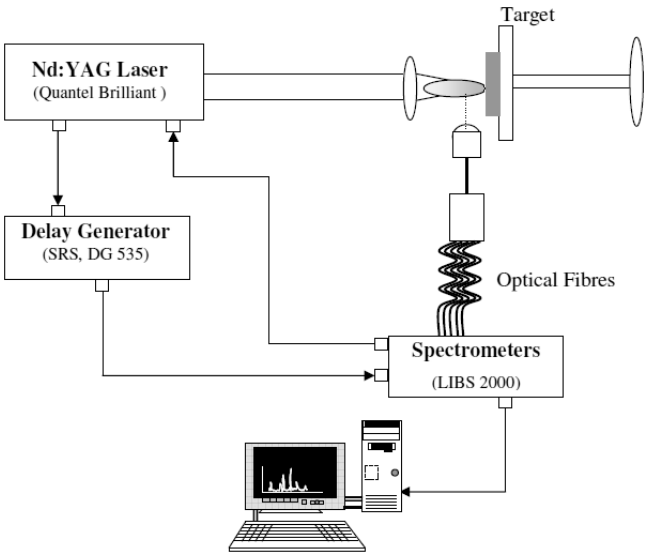

Fig. 2. Schematic diagram of the experimental setup.

The experimental system shown in Fig. 2 is similar to the one described in our previous works [17–22]. Briefly, we use a Q-switched Nd:YAG (Quantel Brilliant) pulsed laser having a pulse duration of 5 ns and 10 Hz repetition rate which is capable of delivering 400 mJ at 1064 nm, and 200 mJ at 532 nm. The laser pulse energy is varied by the flash lamp Q-switch delay through the laser controller, and the pulse energy is measured by a Joule meter (Nova Quantel 01507). The laser beam is focused on the target using a convex lens of 20 cm focal length. The sample is mounted on a 3D sample stage, which is rotated to avoid the nonuniform pitting of the target. The distance between the focusing lens and the sample is kept less than the focal length of the lens to prevent any breakdown of the ambient air in front of the target. The spectra are obtained by averaging 10 data of single shots under identical experimental conditions. The radiation emitted by the plasma is collected by an optical fiber (high OH, core diameter 600 μm) having a collimating lens (0–45° field of view) placed at right angle to the direction of the laser beam. The optical fiber is connected with the LIBS-2000 detection system (Ocean Optics Inc.) to measure the plasma emission. The emission signal is corrected by subtracting the dark signal of the detector through the LIBS software. The LIBS-2000 detection system is equipped with five spectrometers, each having a slit width of 5 μm, covering the range 220–720 nm. Each spectrometer has a 2048-element linear CCD array and an optical resolution of ≈ 0.05 nm by scanning a narrow-bandwidth dye laser. In the experiments, the time delay between the laser pulses and the start of the data acquisition is about 3.5 μs, whereas the system integration time is 2.1 ms. In order to record the emission spectrum, the LIBS-2000 detection system is synchronized with a Q switch of the Nd:YAG laser. The flash lamp out of the Nd:YAG laser triggers the detection system through a four-channel digital delay/pulse generator (SRS DG 535). The LIBS-2000 detection system triggered the Q switch of the Nd:YAG laser.

3. Results and Discussion

3.1. Optical Emission Spectra

In the first set of our experiments, we recorded the plasma emission generated by the fundamental (1064 nm) mode of the Nd:YAG laser. The laser was focused by a quartz lens with a focal length of 20 cm. The potassium plasma was recorded at different positions along the propagation direction of the plasma. Figure 3 shows the emission spectrum taken with the 1064 nm laser. One sees the spectral lines of potassium covering the spectral region 400–700 nm, and the portion of the spectrum predominantly shows the spectral lines of natural potassium. The acquired data are averaged for three laser shorts. The lines at 404.72 nm correspond to the $5p^2P_{1/2} \rightarrow 4s^2S_{1/2}$ transition, 532.32 nm to $8s^2S_{1/2} \rightarrow 4p^2P_{1/2}$, 580.17 nm to $7s^2S_{1/2} \rightarrow 4p^2P_{3/2}$, 691.10 nm to $6s^2S_{1/2} \rightarrow 4p^2P_{1/2}$, and 696.41 nm to $4d^2D_{3/2} \rightarrow 4p^2P_{3/2}$.

A line belonging to Br(I) at 585.20 nm is also seen in the emission spectrum. The line identification is straightforward as the energy levels of potassium are tabulated in the NBS (NIST) database [23].

3.2. Determination of Plasma Parameters

3.2.1. Electron Temperature

We estimate the electron temperature using the Boltzmann plot method under the assumption that the plasma is in local thermodynamic equilibrium (LTE) [24]. We use the following relationship:

$$\ln\left(\frac{I_{ki}\lambda_{ki}}{A_{ki}g_k}\right) = \ln\left(\frac{N(T)}{U(T)}\right) - \frac{E_k}{kT}\,, \tag{1}$$

where I_{ki} is the integrated line intensity of the transition between the upper level k and the lower level i, λ_{ki} is the transition wavelength, A_{ki} is the transition probability, g_k is the statistical weight of level k, $N(t)$ is the total number density, $U(T)$ is the partition function, E_k is the energy of the upper level, k is the Boltzmann constant, and T is the electron temperature. A plot of (1) on the left-hand side against the upper level energy E_k yields a straight line with a slope of $(-1/kT)$. Thus, one can determine the plasma temperature without knowing the total number density or the partition function. The systematic errors are bound to be present; therefore, the temperature is extracted with $\approx 10\%$ accuracy, coming mainly from the transition probabilities and the measurement of the integrated intensity of the spectral lines. We use four K I lines at 404.72, 532.32, 691.10, and 696.41 nm to determine the electron temperature T_e, using the Boltzmann plot method, as shown in Fig. 4.

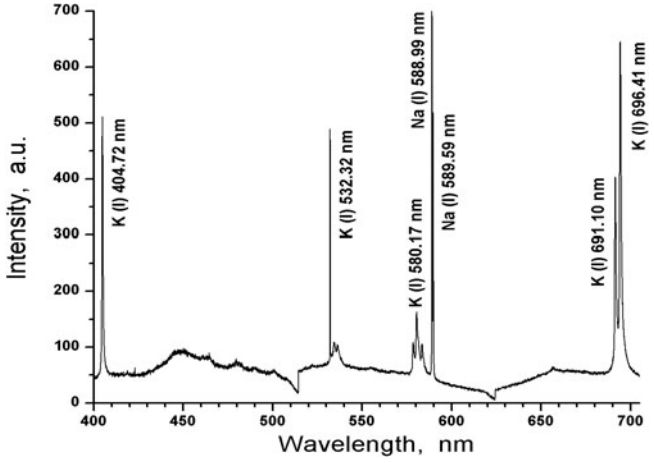

Fig. 3. The emission spectrum of K plasma generated by fundamental harmonic (1064 nm) of the Nd:YAG laser covering the range 400–700 nm.

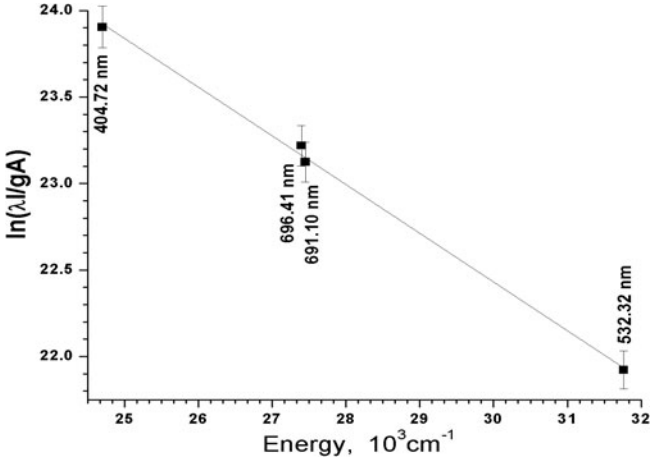

Fig. 4. Boltzmann plot for the K I spectral lines at a distance of 0.05 mm from the target surface using the fundamental mode (1064 nm) of the Nd:YAG laser.

We calculate the electron temperature as a function of the distance from the target surface for both modes of the Nd:YAG laser (1064 and 532 nm), as shown in Fig. 5. In the case of the laser generation at the fundamental (1064 nm) mode, the temperature varies from 5110 to 4130 K, whereas it varies from 4940 to 4030 K in the case of the second-harmonic (532 nm) generation as the distance varies from being close to the target surface 0.05 and up to 2 mm. The electron temperature is also determined by varying the laser irradiance from $2\cdot10^{10}$ for the fundamental (1064 nm) mode to $6.5\cdot10^{10}$ for the second harmonic

(532 nm). The temperature increases from 4320 to 5230 K in the first case, and from 4200 to 5060 K for the second case (see Fig. 6).

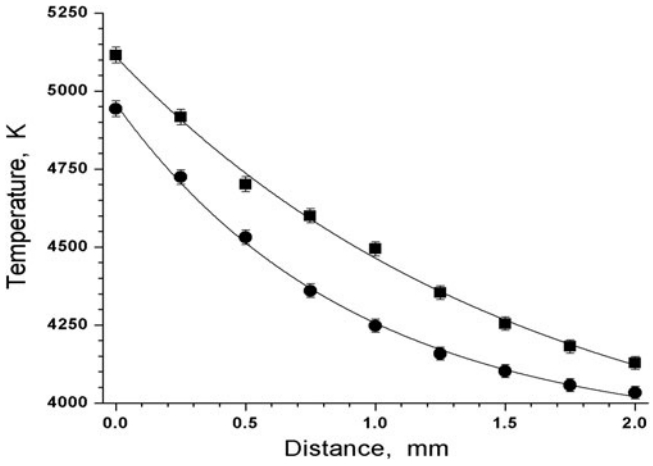

Fig. 5. Variations in the electron temperature along the propagation direction of the plume for the fundamental mode 1064 nm (■) and the second harmonic 532 nm (●) of the Nd:YAG laser.

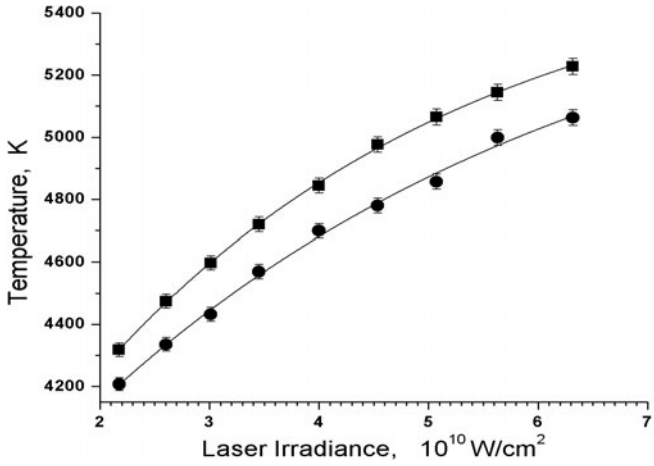

Fig. 6. Variations in the electron temperature with the laser irradiance using the fundamental harmonic 1064 nm (■) and the second harmonic 532 nm (●) of the Nd:YAG laser.

3.2.2. Electron-Number Density

A most reliable technique to determine the electron-number density N_e is connected with the measured Stark-broadened-line profile of an isolated line of either a neutral atom or a single charge ion. Being related to the full width at half maximum (FWHM) of the Stark-broadened lines, it is given by the relation [1–3, 24]

$$\Delta\lambda_{1/2} = 2\omega\left(\frac{N_e}{10^{16}}\right) + 3.5A\left(\frac{N_e}{10^{16}}\right)^{1/4}\left[1 - \frac{3}{4}N_D^{-1/3}\right]\omega\left(\frac{N_e}{10^{16}}\right), \tag{2}$$

where ω is the electron-impact width parameter, A is the ion broadening parameter, N_e is the electron-number density, and N_D is the number of particles in the Debye sphere. The first term in Eq. (2) refers to the broadening due to the electron contribution, whereas the second term is attributed to the ion broadening. Since the contribution of the ionic broadening is normally very small, it can be neglected. Therefore, Eq. (2) reduces to

$$\Delta\lambda_{1/2} = 2\omega\left(\frac{N_e}{10^{16}}\right), \tag{3}$$

where $\Delta\lambda_{1/2}$ is the width of the spectral line, and ω is the impact broadening factor. The values of ω corresponding to different plasma temperatures are adopted from [10].

In Fig. 7, we show the Stark broadened profile of K I line at 532.32 nm obtained with the help of the 1064 nm laser. The full line represents the Lorentzian fit to the experimental data points. The full width at half maximum (FWHM) of the spectra are used to estimate the electron-number density. The condition of the applicability of the Boltzmann plot method for calculating the plasma temperature is the fact that the plasma should be in local thermodynamic equilibrium (LTE), i.e., the equilibrium exists

in a small space domain, and it can differ from domain to domain. The McWhirter criterion [2, 25, 26] satisfies the LTE conditions

$$N_e \geq 1.6 \cdot 10^{12} T^{1/2} (\Delta E)^3. \tag{4}$$

In Eq. (4), $T(K)$ is the electron temperature and ΔE [eV] is the energy difference between the states, which are expected to be in the LTE. At $\sim 5110\,\mathrm{K}$, Eq. (4) yields $N_e \approx 10^{15}$ cm^{-3}. Under these conditions, the contribution due to collisions dominates. The electron-number densities determined in our experiments are within the range to satisfy the LTE conditions. When we focus the laser light on the target, the ablation of the target takes place and, due to the density gradient, the plasma rapidly expands.

The spatial behavior of the electron-number density in the plume is determined in view of Eq. (3). The electron-number density N_e in the case of the fundamental mode (1064 nm) of the Nd:YAG laser with irradiance $6.5 \cdot 10^{10}$ W·cm^{-2} varies from $1.20 \cdot 10^{16}$ to $2.68 \cdot 10^{15}$ cm^{-3}, whereas in the case of the second harmonic (532 nm) it varies from $9.68 \cdot 10^{15}$ to $2.17 \cdot 10^{15}$ cm^{-3} with change in the distance from the target surface from 0 to 2 mm; in both cases, we employ the K I line at 532.32 nm as shown in Fig. 8. We observe that N_e has the maximum value close to the target and decreases with increase in the distance from the target. The temperature and electron-number density both have maximum values close to the target, since the region close to the surface continuously absorbs the laser radiation during the laser pulse.

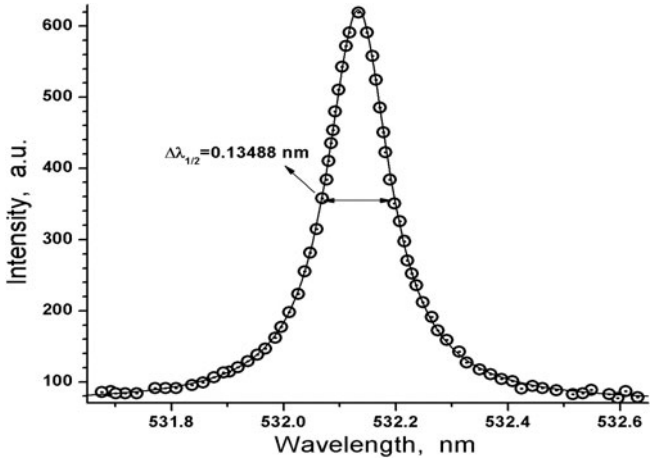

Fig. 7. Stark-broadened profile of K I line at 532.32 nm. The experimental profile (dots) and a Lorentzian fit (the solid curve) with $\Delta\lambda_{1/2} = 0.13488$ nm.

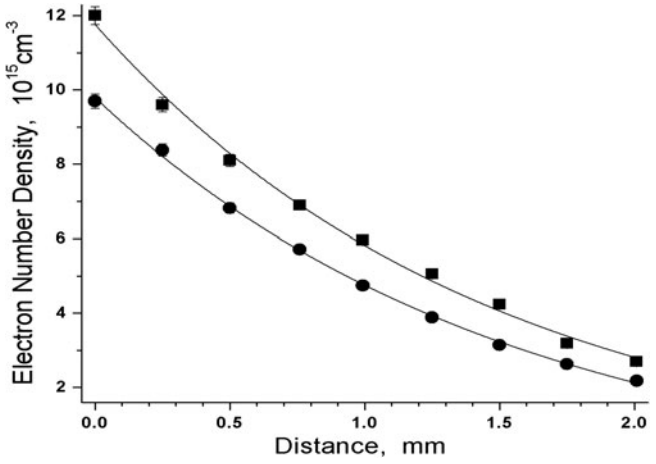

Fig. 8. Variations in the electron-number density with distance from the target for the fundamental mode 1064 nm (■) and the second harmonic 532 nm (●) of the Nd:YAG laser.

When the plasma expands, it thermalizes by transferring the energy to its surroundings. Moreover, it is transparent to the laser pulse; therefore, the temperature and electron-number density decrease along the plume expansion direction. The temperature and electron-number density are different for the fundamental mode and the second harmonic of the Nd:YAG laser, due to the difference in the energy per photon in each regime.

We studied the spatial behavior of the spectrum window at 300–700 nm using the fundamental mode 1064 nm of the Nd:YAG laser, when the distance along the plume was varied from the target surface up to 2 mm in small steps. We observed that the spectrum lines were most intense near the potassium

surface, and their intensities decreased as we moved away from the target surface in the direction of the plume expansion. An identical trend was observed at 532 nm laser wavelength. This variation in the intensity of K lines at the 1064 nm laser irradiation due to changing the distances is shown in Fig. 9.

3.3. Effect of the Laser Irradiance

We determined the electron-number density for different values of the laser irradiance. In both regimes of the Nd:YAG laser generation, we observed an identical trend in the variation in the electron-number density as a function of the laser irradiance. The variation in the electron-number density with the laser irradiance also shows a similar behavior. Figure 10 shows the variation in the electron-number density as a function of the laser irradiance in the regime of laser operation at the fundamental mode (1064 nm), in which the laser irradiance varies from $2 \cdot 10^{10}$ to $6.5 \cdot 10^{10}$ W·cm^{-2} and the corresponding electron-number densities vary from $1.20 \cdot 10^{15}$ to $8.90 \cdot 10^{15}$ cm^{-3}.

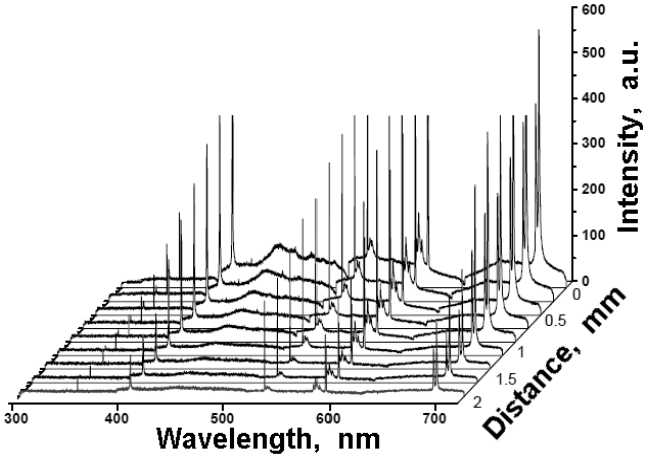

Fig. 9. Spatial behavior of the spectrum lines of potassium along the direction of the plasma-plume propagation using the laser at 1064 nm with irradiance of $4.6 \cdot 10^{10}$ W/cm^2.

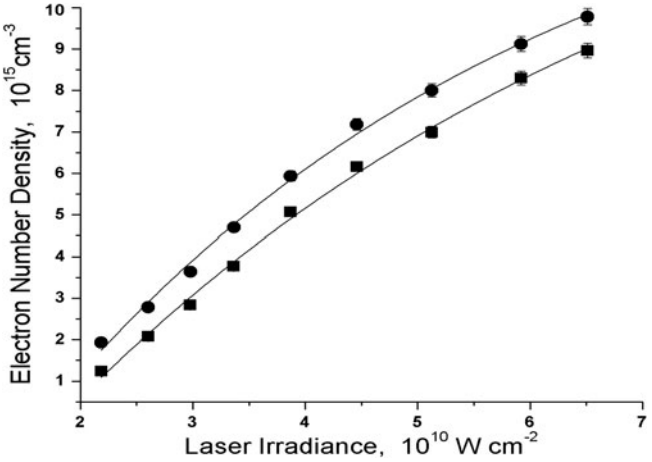

Fig. 10. Variations in the electron-number density with changes in the laser irradiance using the fundamental mode 1064 nm (■) and the second harmonic 532 nm (●) of the Nd:YAG laser.

In the case of laser operation at the second harmonic (532 nm), the electron-number density varies from $1.95 \cdot 10^{15}$ to $9.75 \cdot 10^{15}$ cm^{-3}. The observed increase in N_e and T_e due to the increase in the laser irradiance is due to the absorption and/or reflection of the laser photons by the plasma, which depends upon the plasma frequency. In our experiment, for both regimes of Nd:YAG laser operation, the corresponding frequencies are $2.8 \cdot 10^{14}$ and $5.6 \cdot 10^{14}$ Hz, respectively, whereas the plasma frequency $\nu_p = 8.9 \cdot 10^3 \sqrt{N_e}$. Since the electron-number density $N_e \approx 10^{16}$ cm^{-3}, $\nu_p = 3.6 \cdot 10^{12}$ Hz, which is less than the laser frequency ($\approx 10^{14}$ Hz), and this fact demonstrates that the energy losses due to the reflection of the laser light from the plasma is insignificant.

4. Conclusions

We used a Q-switched Nd:YAG laser at the fundamental mode (1064 nm) and the second harmonic (532 nm) to study the laser-produced potassium plasma. The emission spectrum of the plasma reveals

transitions of potassium. We determined the electron temperature T_e and the electron-number density N_e along the axial positions of the plasma plume. We observed that the spatial behavior of the electron temperature and electron-number density close to the target have the maximum values and decrease along the distance from the target. Variations in the electron temperature and electron-number density with the laser irradiance show that both parameters increase with increase in the laser irradiance. The electron temperature calculated for the fundamental mode (1064 nm) of the Nd:YAG laser is 5110 K, and that for the second harmonic (532 nm) is 4940 K. The electron-number density close to the target in the case of the fundamental mode (1064 nm) of the Nd:YAG laser is $1.20 \cdot 10^{16}$ cm^{-3}, and in the case of the second harmonic (532 nm) it is $9.68 \cdot 10^{15}$ cm^{-3}. The plasma parameters that we determined, up to our knowledge, are reported the first time using the LIBS technique; the previous investigations of potassium [8–16] were related to other aspects.

References

1. A. W. Miziolek, V. Palleschi and I. Schechter, *Laser-Induced Breakdown Spectroscopy (LIBS)*, Cambridge University Press (2006).
2. D. A. Cremers and L. J. Radziemski, *Handbook of Laser-Induced Breakdown Spectroscopy*, John Wiley, New York (2006).
3. J. P. Singh and S. N. Thakur, *Laser-Induced Breakdown Spectroscopy*, Elsevier, USA (2007).
4. C. Pasquini, J. Cortez, L. M. C. Silva, and F. B. Gonzaga, *J. Braz. Chem. Soc*, **18**, 463 (2007).
5. E. F. Runge, R. W. Minck, and F. R. Bryan, *Spectrochim. Acta*, **20**, 733 (1964).
6. D. A. Rusak, B. C. Castle, B. W. Smith, and J. D. Winefordner, *Trends Anal. Chem.*, 11 (1998).
7. B. Nemet and L. Kozma, *Spectrochim. Acta B*, **50**, 1869 (1995).
8. R. M. Measures, *J. Quantum Spectrosc. Radiat. Transfer*, **10**, 107 (1970).
9. G. E. Thomas, R. J. Hott, D. Boyer, et al., *Nucl. Instrum. Meth. A*, **257**, 32 (1987).
10. N. Konjevic and W. L. Wiese, *J. Phys. Chem. Ref. Data*, **19**, 1307 (1990).
11. S. Yilmaz, T. Venkatesan, and R. Multhaupt Gerhard, *Appl. Phys. Lett.*, **58**, 2479 (1991).
12. J. J. E. Reid, *Appl. Phys. Lett.*, **62**, 19 (1993).
13. W. V. Davis, M. Kauranen, E. M. Nagasako, et al., *Phys. Rev. A*, **5**, 4152 (1995).
14. U. V. Zahn and J. Hoffner, *Geophys. Res. Lett.*, **23**, 141 (1996).
15. M. J. Nystrom, B. W. Wessels, J. Chen, and T. J. Marks, *Appl. Phys. Lett.*, **68**, 761 (1996).
16. V. Wascotte, P. Caspers, J. de Sterke, et al., *Pharm. Res.*, **24**, 1897 (2007).
17. M. Hanif, M. Salik, and M. A. Baig, *J. Plasma Sci. Tech.*, **13**, 129 (2011).
18. M. Salik, M. Hanif, and M. A. Baig, *IEEE Trans. Plasma Sci.*, **36**, 1861 (2011).
19. M. Hanif, M. Salik, and M. A. Baig, *J. Opt. Laser Eng.*, **49**, 1456 (2011).
20. M. Hanif, M. Salik, and M. A. Baig, *J. Appl. Phys. B*, DOI 10.1007/s00340-012-5293-1 (2012).
21. M. Hanif, M. Salik, and M. A. Baig, *Opt. Spectrosc.*, **114**, 7 (2013).
22. S. Hafeez, N. M. Sheikh, and M. A. Baig, *Laser Part. Beams*, **26**, 41 (2008).
23. Kurucz output atomic spectra line database from R. L. Kurucz's CD-ROM 23, *NIST Atomic Spectra Database* [http://physics.nist.gov].
24. H. R. Griem, *Principles of Plasma Spectroscopy*, Cambridge University Press (1997).
25. R. W. P. McWhirter, in: R. H. Huddlestone and S. L. Leonard (Eds.), *Plasma Diagnostic Techniques*, Academic Press, New York (1965).
26. O. Barthélemy, J. Margot, S. Laville, et al., *Appl. Spectrosc.*, **59**, 529 (2005).